3WC-GBNRS++: A Novel Three-Way Classifier With Granular-Ball Neighborhood Rough Sets Based on Uncertainty

Jie Yang, Zhuangzhuang Liu, Shuyin Xia, *Member, IEEE*, Guoyin Wang, *Senior Member, IEEE*, Qinghua Zhang, *Senior Member, IEEE*, Shuai Li, and Taihua Xu

***Abstract*—Three-way decision with neighborhood rough sets (3WDNRS) is adept at addressing uncertain problems involving continuous data by configuring the neighborhood radius. However, on one hand, the inputs of 3WDNRS are individual neighborhood granules, which reduce the decision efficiency and generality; on other hand, the thresholds of 3WDNRS require prior knowledge to be approximately set in advance, making it difficult to apply in cases where such knowledge is unavailable. To address these issues, we introduce granular-ball computing into 3WDNRS from the perspective of uncertainty. First, we propose an enhanced granular-ball generation method based on DBSCAN called DBGBC. Subsequently, we present an improved granular-ball neighborhood rough sets model (GBNRS++) by combining DBGBC with a quality index. Furthermore, we construct a three-way classifier with granular-ball neighborhood rough sets (3WC-GBNRS++) based on the principle of minimum fuzziness loss. This approach provides an objective and efficient way to determine the thresholds. To further enhance classification accuracy, we design an adaptive granular-ball neighborhood within the subsequent classification process of 3WC-GBNRS++. Finally, experimental results demonstrate that, 3WC-GBNRS++ almost outperformed other comparison methods in terms of effectiveness and robustness, including four state-of-the-art granular-balls-based classifiers and five classical machine learning classifiers on 12 public benchmark datasets. Moreover, we discuss the limitations of our work and the outlook for future research.**

Manuscript received 31 January 2024; revised 30 March 2024; accepted 3 May 2024. Date of publication 7 May 2024; date of current version 6 August 2024. This work was supported in part by the National Science Foundation of China under Grant 62066049, Grant 62221005, and Grant 62176070, in part by the Guizhou Provincial Department of Education Colleges and Universities Science and Technology Innovation Team under Grant QJJ[2023]084, in part by the Science and Technology Top Talent Project of Guizhou Education Department under Grant QJJ2022[088], and in part by the Excellent Young Scientific and Technological Talents Foundation of Guizhou Province (QKH-platform talent under Grant (2021) 5627). Recommended by Associate Editor W. Ding. *(Corresponding author: Taihua Xu.)*

Jie Yang is with the School of Physics and Electronic Science, Zunyi Normal University, Zunyi 563002, China, and with the School of Computer, Jiangsu University of Science and Technology, Zhenjiang 212100, China, and also with the Chongqing Key Laboratory of Computational Intelligence, Chongqing University of Posts and Telecommunications, Chongqing 400065, China (e-mail: yj530966074@foxmail.com).

Zhuangzhuang Liu and Taihua Xu are with the School of Computer, Jiangsu University of Science and Technology, Zhenjiang 212100, China (e-mail: Just_Liuzz@163.com; xth19890410@163.com).

Shuyin Xia, Guoyin Wang, Qinghua Zhang, and Shuai Li are with the Chongqing Key Laboratory of Computational Intelligence, Chongqing University of Posts and Telecommunications, Chongqing 400065, China (e-mail: xiasy@cqupt.edu.cn; wanggy@cqupt.edu.cn; zhangqh@cqupt.edu.cn; zorro0311@126.com).

Digital Object Identifier 10.1109/TFUZZ.2024.3397697

***Index Terms*—Adaptive granular-ball (GB) neighborhood, granular-ball neighborhood rough sets (GBNRS), fuzziness loss, three-way classifier with granular-ball neighborhood rough sets (3WC-GBNRS++), three-way decision (3WD).**

I. Introduction

THREE-WAY decision (3WD) [1], [2], [3] is an emerging approach that addresses the complex problem with uncertainty. The threshold pair $[\beta, \alpha]$ in 3WD is used to divide a universe into three pairwise disjoint regions, namely, the positive region, negative region, and boundary region, respectively. Building on the traditional two-way decision model, 3WD introduces a third option, providing a trisecting-and-acting method for decision-making. Granular computing (GrC) [2], [4], [5], simulating human cognitive mechanisms, offers a formidable tool for addressing complex problem-solving and managing uncertain information by emphasizing a multifaceted understanding and description of the real world across multiple levels and perspectives. GrC has has a wide range of applications in numerous fields, including bidirectional cognitive computing models [6], 3WD [7], multigranularity joint problem-solving mechanisms [8], etc. Based on the idea of GrC, Yao [9] further developed sequential 3WD (S3WDs). Essentially, S3WD is a progressive computational method with multigranularity spaces. Recently, by integrating related theories, i.e., concept lattice [8], rough sets [7], and fuzzy sets [10], significant progress has been made in 3WD and resulting in its widespread application in various domains, including classification [11], multilabel learning [12], clustering analysis [13], deep learning [14], group decision-making [15], etc.

To reduce the decision risk for approximating an uncertain concept, 3WD with Palwak rough sets theory is defined based on equivalence relation. To process continuous data, neighborhood rough sets (NRS) [16] employ neighborhood relations to partition a universe. Three-way decision with NRS (3WDNRS) [17] is proposed to construct the three-way neighborhood space based on the basic neighborhood granules. Currently, there are also many research investigations on 3WDNRS in a wide range of areas. Huang [18] proposed a generalized 3WDNRS by assigning the interval-valued loss function to each object for incomplete information system. Ye [19] established a probabilistic rough fuzzy sets model and multicriteria decision-making-based 3WD model by using the created fuzzy-neighborhood

classes. Yang [20] conducted a study on a S3WD strategy that integrates multigranularity in neighborhood system. Chu [21] introduced a three-way clustering algorithm utilizing NRS to enhance decision-making efficiency. However, the inputs of current works on 3WDNRS are individual neighborhood granules, which reduce the decision efficiency and generality. Moreover, in practical applications, it is extremely challenging to accurately acquire risk parameters using known decision information. Consequently, the thresholds are determined subjectively depending on the judgement of experts. That is, the thresholds require a priori knowledge to be approximately set in advance; they are unable to function effectively in scenarios where such knowledge is unavailable.

Granular-ball computing (GBC) [22], [23] is a novel method that replaces traditional information granule with GB for data processing and knowledge representation. As a multigranularity representation and computation theory, GBC has evolved in terms of methods and applications, and basic theories, such as GB clustering [24], GB classifier [25], [26], GB neural network [27], GB evolutionary computation [28], and GB fuzzy set [29], have been established. Chen [30] introduced a GB-based attribute selector that enhances classification performance. Zhang [31] proposed a dynamic update mechanism based on GBC. This approach focuses on update of GBs by considering the changes in their quality. Recently, Xia [32] introduced the novel concept of GBNRS, which integrates ideas from both GBC and NRS. GBNRS offers greater robustness and efficiency by replacing neighborhood granules with GBs. In particular, noisy objects are less likely to impact the performance of GBs, due to their coarse-grained features. Moreover, compared to traditional granules, GBs serve as sample points that more accurately represent multigranularity knowledge concepts and capture the overall data distribution, which aligns with human large-scale cognition. For example, as a classical tool to deal with uncertainty problems, fuzzy rough set [33] is able to process continuous data and has been extensively studied [34], [35], [36]. Due to the use of fuzzy binary relations to represent the similarity between samples in fuzzy rough set, numerical attribute values no longer need to be discretized. However, compare with GBNRS, the inputs of fuzzy rough set are individual fuzzy information granules, which reduces the decision efficiency and generality. Moreover, fuzzy rough set lacks an effective knowledge representation capability due to the fact that its information granules are comprised of sample points, while GBNRS provides an improved interpretability. However, although GBNRS has greater robustness and reduces the time complexity, there are still some limitations in current GBNRS as follows.

1) The quality of GBC primarily depends on the purity, resulting in some potential misclassification in neighborhood classifier based on GBNRS.
2) GBNRS utilizes the classic two-way decision approach and assigns the label of the nearest GB to predicted sample, which may lead to risky classification on uncertain problems.

Based on the discussion, this article further enhances the performance of GBNRS by improving the generation and measure of GBs, named GBNRS++. Moreover, we introduce GBNRS++ into 3WD to construct the three-way classifier with granular-ball neighborhood rough sets (3WC-GBNRS++). The core of 3WC-GBNRS is to calculate threshold pair to divide a GB space into three pairwise disjoint regions for classification. Compared to traditional 3WDNRS methods, 3WC-GBNRS++ has the following advantages.

1) In 3WC-GBNRS++, an improved GB generation method based on the DBSCAN algorithm (DBGBC) to address the subdivision degree of GBs, which avoids the potential errors in subsequent classification process.
2) 3WC-GBNRS++ is constructed based on minimum fuzziness loss, which avoids the subjective definition of certain risk parameters when calculating the thresholds. This parameter-free characteristic of 3WC-GBNRS++ results in better generalizability in comparison with 3WDNRS.
3) To further enhance the classification accuracy, an adaptive GB neighborhood is designed for predicted objects in subsequent classification process of 3WC-GBNRS++.

The rest of this article is organized as follows. Section II is a review of related preliminary definitions. In Section III, we discuss the disadvantages of GBC and present an improved granular-ball neighborhood rough sets (GBNRS++). Section IV presents the 3WC-GBNRS++ is constructed based on uncertainty. In Section V, the relevant experiments for the verification and evaluation of our proposed methods are shown. Finally, Section VI concludes this article.

II. Preliminaries

In this section, to facilitate the framework of this article, we review some necessary definitions related to 3WD, NRS, and GBC, etc. Let NS $= (U, C \cup D, V, f)$ represent a neighborhood decision system, where $U = \{x_1, x_2, \ldots, x_N\}$ is the universe of discourse; C and D are the nonempty finite sets of conditional attributes and decision attributes, respectively; V is the set of values of attributes; $f : U \times C \to V$ denotes a mapping function.

Definition 1 (NRS [16], [17]): Given a neighborhood decision system NS $= (U, C \cup D, V, f)$, $\forall R \subseteq C$ and $X \subseteq U$, the lower and upper approximations of X with respect to R defined as follows:

$$\underline{NR}(X) = \{x \mid \delta_R(x) \subseteq X, x \in U\} \tag{1}$$

$$\overline{NR}(X) = \{x \mid \delta_R(x) \cap X \neq \phi, x \in U\} \tag{2}$$

where $\delta_R(x) = \{x \mid \Delta(x, x_k) \leq \delta, x_k \in U\}$ and $\Delta(x, x_k)$ represents the distance between x and x_k, and δ denotes the neighborhood radius.

Definition 2 (Fuzziness [37]): Let $F(U)$ be the family of all fuzzy sets on U, M, and N be any two distinct fuzzy sets on U. A mapping $H : F(U) \to [0, 1]$ denotes the fuzziness of a fuzzy set. The function H must satisfy the following conditions.

(1) $H(M) = 0$, iff $M \in P(U)$, where $P(U)$ is a power set of U.
(2) $H(M) = 1$, iff $\forall x_i \in U, M(x_i) = \frac{1}{2}$.
(3) $H(M) \geq H(N)$, iff $\forall x_i \in U, N(x_i) \geq M(x_i) \geq \frac{1}{2}$ or $N(x_i) \leq M(x_i) \leq \frac{1}{2}$.

Definition 3 (Average fuzzy set [38]): Given a neighborhood decision system denoted as NS $= (U, C \cup D, V, f)$, $R \subseteq C$ and $X \subseteq U$. The set X represents a target subset of U. $\mu(t)$ denotes the membership of an object t, where $t \in \delta_R(x)$, then $\bar{\mu}(x)$ represents the average membership of $\delta_R(x)$

$$\bar{\mu}(x) = \frac{\sum_{t \in \delta_R(x)} \mu(t)}{|\delta_R(x)|}. \tag{3}$$

Then, the average fuzzy set of X is represented as follows:

$$X_R^J = \frac{\bar{\mu}(x_1)}{x_1} + \frac{\bar{\mu}(x_2)}{x_2} + \cdots + \frac{\bar{\mu}(x_N)}{x_N}. \tag{4}$$

Definition 4 (Average fuzziness [38]): Given a neighborhood decision system NS $= (U, C \cup D, V, f)$, $R \subseteq C$ and $X \subseteq U$. The average fuzziness of x is defined as $h(x) = 4\bar{\mu}(x)(1 - \bar{\mu}(x))$.

When U is a discrete universe, the definition of the average fuzziness of X_R^J is represented by

$$H_{X_R^J} = \frac{1}{|U|} \sum_{x \in U} h(x). \tag{5}$$

When U is a continuous universe on $[a, b]$, the definition of the average fuzziness of X_R^J is represented by

$$H_{X_R^J} = \frac{1}{|b-a|} \int_a^b h(x) dx. \tag{6}$$

Definition 5 (See [25]): Given a neighborhood decision system NS $= (U, C \cup D, V, f)$, GBs $= \{\text{GB}_1, \text{GB}_2, \ldots, \text{GB}_n\}$ is a GB space generated on NS by GBC. $R \subseteq C$ and $X \subseteq U$, $\forall \text{GB}_i \in$ GBs, c_i and r_i represent the center and radius of GB_i, respectively, defined as follows:

$$c_i = \frac{1}{N} \sum_{x \in \text{GB}} x \tag{7}$$

$$r_i = \frac{1}{N} \sum_{x \in \text{GB}} \|x - c_i\| \tag{8}$$

where c_i is the center of gravity calculated as the average of all objects in GB_i, and r_i is the average distance from each point in GB_i to c_i.

Definition 6 (See [25]): Given a neighborhood decision system NS $= (U, C \cup D, V, f)$, GBs $= \{\text{GB}_1, \text{GB}_2, \ldots, \text{GB}_n\}$ is a GB space generated on NS by GBC, $\forall \text{GB}_i \in$ GBs. Let O be a test point, and the distance from O to GB_i is denoted as $\text{dis}(O, \text{GB}_i)$, defined as follows:

$$\text{dis}(O, \text{GB}_i) = \begin{cases} \text{dis}(O, c_i) - r_i, & \text{if } \text{dis}(O, c_i) - r_i > 0 \\ 0, & \text{else.} \end{cases} \tag{9}$$

Definition 7 (See [25]): Given a neighborhood decision system NS $= (U, C \cup D, V, f)$, GBs $= \{\text{GB}_1, \text{GB}_2, \ldots, \text{GB}_n\}$ is a GB space generated on NS by GBC. $\forall \text{GB}_i \in$ GBs, the overall label of GB_i is defined as the majority label of GB_i, denoted by $l(\text{GB}_i)$.

From Definition 3, it is easy to obtain the average membership of a GB GB_i as follows:

$$\bar{\mu}(\text{GB}) = \frac{\sum_{x \in \text{GB}_i} \mu(x)}{|\text{GB}_i|}. \tag{10}$$

Based on GBC, the GBNRS [32] is further proposed, which is defined as follows.

Definition 8 (See [32]): Given a neighborhood decision system NS $= (U, C \cup D, V, f)$, GBs $= \{\text{GB}_1, \text{GB}_2, \ldots, \text{GB}_n\}$ is a GB space generated on NS by GBC. $R \subseteq C$ and $X \subseteq U$, $\forall \text{GB}_i \in$ GBS, the lower approximation, upper approximation, and generation lower approximation of X with respect to R defined as follows:

$$\underline{G_R}(X) = \{x \in U \mid x \in \text{GB}_i, \bar{\mu}(\text{GB}_i) \geq \alpha\} \tag{11}$$

$$\overline{G_R}(X) = \{x \in U \mid x \in \text{GB}_i, \bar{\mu}(\text{GB}_i) > \beta\} \tag{12}$$

$$\underline{G'_R}(X) = \{c_i \mid \bar{\mu}(\text{GB}_i) \geq \alpha\}. \tag{13}$$

Accordingly, the rules for dividing the three decision regions based on $\bar{\mu}(\text{GB}_i)$ are defined as

$$\text{POS}_R^{(\beta,\alpha)}(X) = \underline{G_R}(X) \tag{14}$$

$$\text{NEG}_R^{(\beta,\alpha)}(X) = U - \underline{G_R}(X) \tag{15}$$

$$\text{BND}_R^{(\beta,\alpha)}(X) = \overline{G_R}(X) - \underline{G_R}(X). \tag{16}$$

Definition 9 (3WD rules [1]): For a given threshold pair (α, β), the 3WD rules are defined as follows.

1) $x \in \text{POS}_R^{(\beta,\alpha)}(X)$, iff $\bar{\mu}(x) \geq \alpha$.
2) $x \in \text{NEG}_R^{(\beta,\alpha)}(X)$, iff $\beta < \bar{\mu}(x) < \alpha$.
3) $x \in \text{BND}_R^{(\beta,\alpha)}(X)$, iff $\bar{\mu}(x) \leq \beta$.

Each object can be assigned into corresponding regions according to their average membership.

III. Improved GB Neighborhood Rough Sets

In the process of generating GBs, Algorithm S1 in Section S1 of supplementary file introduces a purity threshold as a parameter to control the granularity. The purity threshold plays a crucial role in controlling the degree of granularity in the division of these GBs. The purity of a GB can be determined by calculating the proportion of the majority label. If the purity of a GB falls below the purity threshold, it will be divided again. Therefore, the higher the purity threshold, the higher the purity of the final generated GBs.

However, there are two limitations as follows. 1) For a GB, the purity is failed to comprehensively measure its robustness, effectiveness, and stability. 2) When the purity threshold is equal to 1 may lead to an unbalanced distribution of data within the partitioned GBs. This means that the performance of GBs needs to be further enhanced. For example, in Fig. 1(a), although the purity of gb_1 and gb_2 is all equal to 1, they exhibit distinct differences in performance. Compared to gb_2, gb_1 has a higher density with the same radius, making it potentially more effective and robust. Moreover, even though the purity of gb_3 is lower than that of gb_2, it is difficult to intuitively observe that gb_2 is necessarily better than gb_3 in terms of performance

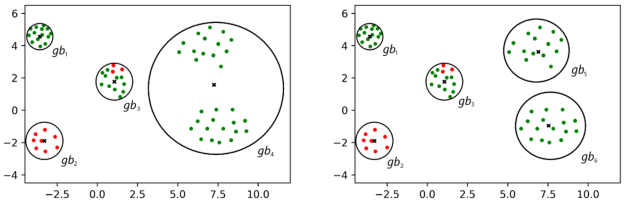

Fig. 1. Generated GBs using GBC and DBGBC on the same dataset. (a) GBC. (b) DBGBC.

because gb_3 has a higher density. The distribution of objects is compactly distributed at the top and bottom of gb_4, which should be further subdivided into two more reasonable GBs gb_5 and gb_6 at the top and bottom, respectively. To solve the above problems, a density-based generation method is first presented to optimize the quality measure of GBs. In addition, a quality index is proposed to measure the performance of GBs. Then, based on the generative GBs and quality measure, we define GBNRS++.

As well known, DBSCAN [39] is a noteworthy density-based clustering algorithm. Unlike partitioning and hierarchical clustering methods, DBSCAN identifies clusters as the maximum set of points that are density-connected. This approach effectively divides regions with high density into clusters and reveals clusters of any shape within a noisy spatial database. The objective of DBSCAN is to discover the largest set of density-connected objects. In this article, we propose a density-based GBs generation method based on DBSCAN as shown in Algorithm 1, named DBGBC. The purity threshold and refined threshold play a pivotal role in determining the granularity quality in Algorithm 1. These thresholds exhibit similarities to coverage or specificity metrics of justifiable granularity, offering a more tailored and specific evaluation for GB generation. The purity threshold serves as a metric that quantifies internal consistency within each GB. To prevent objects from different classes from being classified under the same label, the purity threshold is set to 1 for generating GBs. In addition, the DBSCAN with refined threshold is utilized to determine whether the distribution of data points is balanced. When the number of cluster centers calculated by DBSCAN in a GB is greater than or equal to 2, it indicates that the distribution of objects in this granule-ball is unbalanced. Therefore, according to the new cluster center and its number, this granule-ball will be further subdivided.

Using DBSCAN algorithm, Algorithm 1 achieves the further subdivision of the previous level of GBs. The original GBs are generated by the purity threshold and the DBSCAN is used to achieve a more balanced and reasonable distribution of objects in each GB. This means that the GBs generated by Algorithm 1 are more reasonable for subsequent classification tasks than Algorithm S1. As shown in Fig. 1(b), it is obviously that Algorithm 1 divides the rightmost original GB gb_4 again and obtains two reasonable GBs gb_5 and gb_6.

The efficiency of Algorithm 1 is explained as follows. Getting GB obtained by Algorithm S1 requires $O(kN^2)$. Calculating the number of new cluster centers and deciding whether to further split the GB using the 2-means requires at most k iterations, requiring $O(kN)$. Here k represents the iteration number, and the sum of elements is represented by N. Thus, the time complexity of Algorithm 1 is still $O(kN^2)$.

Algorithm 1: The Density-based Granular-balls Generation Method Based on DBSCAN.

Input: GB_list obtained by Algorithm S1
Output: The set of density-based granular balls $DBGB\_list$

Initialize $DBGB\_list = \{\}$;
Function `Split_DBGB(`GB`)`**:**
  Calculate the number of new cluster centers of GB using DBSCAN algorithm;
  if *the number of new cluster centers of* GB *is less than 2* **then**
    Add GB to the $DBGB\_list$;
  end
  else
    $GB_1, GB_2 \leftarrow GB$ is subdivided into two granular balls by 2-means clustering algorithm using the new cluster centers;
    `Split_DBGB(`GB_1`)`;
    `Split_DBGB(`GB_2`)`;
  end
return
Function `Main(`GB_list`)`**:**
  for GB_i *in* GB_list **do**
    `Split_DBGB(`GB_i`)`;
  end
  return $DBGB\_list$;
return

Definition 10 (Quality index): Let GBs $= \{\mathrm{GB}_1, \mathrm{GB}_2, \ldots, \mathrm{GB}_n\}$ be a GB space. The quality index of GB_i, denoted as $m(\mathrm{GB}_i)$, is expressed as follows:

$$m(\mathrm{GB}_i) = \frac{p_i \times (\rho_i + 1)}{2} \tag{17}$$

where p_i denotes the purity of GB_i, $\rho_i = \sum_{j \neq i} \exp\left[-\left(\frac{d_{ij}}{d_c}\right)^2\right]$ represents the local density of GB_i. d_c is a constant taken as 1%–2% of the total objects. d_{ij} represents the distance between the center of GB_i and object x_j within GB_i.

Then, the average fuzzy set of X based on GBs is represented as follows:

$$\mathbb{X}_{\mathbb{R}}^{\mathbb{J}} = \frac{m(\mathrm{GB}_1)}{c_1} + \frac{m(\mathrm{GB}_2)}{c_2} + \cdots + \frac{m(\mathrm{GB}_n)}{c_n}. \tag{18}$$

From Definition 4, we have the definition of the average fuzziness of GBs based on formula (17) as follows.

Definition 11: Given a neighborhood decision system NS $= (U, C \cup D, V, f)$, GBs $= \{\mathrm{GB}_1, \mathrm{GB}_2, \ldots, GB_n\}$ is a GB space generated on NS. $R \subseteq C$ and $X \subseteq U$. The average fuzziness of $\mathbb{X}_{\mathbb{R}}^{\mathbb{J}}$ is represented by

$$H_{\mathbb{X}_{\mathbb{R}}^{\mathbb{J}}} = \frac{1}{|U|} \sum_{\mathrm{GB} \in \mathrm{GBs}} \xi(\mathrm{GB}) \tag{19}$$

where $\xi(\text{GB}) = 4m(\text{GB})(1 - m(\text{GB}))$.

According to Definition 11, the average fuzziness of $\mathbb{X}_{\mathbb{R}}^{\mathbb{J}}$ essentially reflects the uncertainty of a GB space. We further define an GBNRS++ as follows.

Definition 12: Given a neighborhood decision system $\text{NS} = (U, C \cup D, V, f)$, $\text{GBs} = \{\text{GB}_1, \text{GB}_2, \ldots, \text{GB}_n\}$ is a GB space generated on NS by DBGBC. (β, α) denotes a threshold pair. $R \subseteq C$ and $X \subseteq U$, $\forall \text{GB}_i \in \text{GBS}$, the lower approximation, upper approximation and generation lower approximation of X with respect to R are defined as follows:

$$\underline{\mathbb{G}}(X) = \{x \in U \mid x \in \text{GB}_i, m(\text{GB}_i) \geq \alpha\} \tag{20}$$

$$\overline{\mathbb{G}}(X) = \{x \in U \mid x \in \text{GB}_i, m(\text{GB}_i) > \beta\} \tag{21}$$

$$\underline{\mathbb{G}'}(X) = \{c_i \mid x \in \text{GB}_i, m(\text{GB}_i) \geq \alpha\}. \tag{22}$$

Accordingly, the rules for dividing the three decision regions are defined as

$$\mathbb{POS}_R^{(\beta,\alpha)}(X) = \underline{\mathbb{G}}(X) \tag{23}$$

$$\mathbb{NEG}_R^{(\beta,\alpha)}(X) = U - \underline{\mathbb{G}}(X) \tag{24}$$

$$\mathbb{BND}_R^{(\beta,\alpha)}(X) = \overline{\mathbb{G}}(X) - \underline{\mathbb{G}}(X). \tag{25}$$

IV. Three-Way Learning With GBNRS Based on Uncertainty

Current 3WD with minimum cost is achieved based on the three regions calculated using the given risk parameters in 3WDNRS. Within the general 3WD framework proposed by Yao et al. [2], the current works in 3WD can be summarized into three aspects: minimum distance, minimum cost, and uncertainty invariance. Our proposed GBNRS++ may introduce more decision-making errors due to its two-way decision-making approach. In addition, this may lead to an uncertainty loss when compared to its corresponding 3WD classifier model. In this article, the fuzziness measure is introduced into GBNRS++ to construct 3WC-GBNRS++ with the adaptive threshold pairs. This introduces a novel approach to 3WD theory from a different perspective.

By utilizing fuzzy-rough transformation, the shadowed sets [40], [41], [42] can be regarded as a three-way approximation of fuzzy sets. The threshold pairs for constructing the shadowed set are calculated by the data itself, avoiding the subjective error caused by the given threshold pairs. Within shadowed sets, objects with membership degrees below α^* and above β^* are assigned to shadowed areas. Based on this, the value range is extended to the uncertain area $[\beta^*, \alpha^*]$ to establish three-way approximations with shadowed sets (3WA-SS) using GBs, which is defined as follows.

Definition 13: Given a neighborhood decision system $\text{NS} = (U, C \cup D, V, f)$, $\text{GBs} = \{\text{GB}_1, \text{GB}_2, \ldots, \text{GB}_n\}$ is a GB space generated on NS by DBGBC. $R \subseteq C$ and $X \subseteq U$. Let a mapping $\psi : \mathbb{X}_{\mathbb{R}}^{\mathbb{J}} \to \{0, [\beta^*, \alpha^*], 1\}$ to represent the three-way approximations of $\mathbb{X}_{\mathbb{R}}^{\mathbb{J}}$ with a shadowed set. Specifically, the mapping ψ is from $\mathbb{X}_{\mathbb{R}}^{\mathbb{J}}$ to set $\{0, [\beta^*, \alpha^*], 1\}$, and $\psi(\mathbb{X}_{\mathbb{R}}^{\mathbb{J}})$ is defined as follows:

$$\psi\left(\mathbb{X}_{\mathbb{R}}^{\mathbb{J}}\right) = \begin{cases} 0, & m(\text{GB}_i) \leq \beta^* \\ [\beta^*, \alpha^*], & \beta^* < m(\text{GB}_i) < \alpha^* \\ 1, & m(\text{GB}_i) \geq \alpha^* \end{cases}$$

where, $i = 1, \ldots, n$.

The boundary region of the interval shadowed sets defined in Definition 13 is represented by an interval, which is a classic form. The process of deriving thresholds in Definition 13 is availability by a data-driven form, because it has stronger rationality and interpretability.

First, we compute the average membership of GB_i ($\text{GB}_i \in \text{GBs}$), forming the average fuzzy set based on GBs $\mathbb{X}_R^J$. Subsequently, a three-way approximation $\psi(\mathbb{X}_{\mathbb{R}}^{\mathbb{J}})$ is applied to $\mathbb{X}_R^J$ as follows.

1) When $m(\text{GB}_i) \leq \beta^*$, $m(\text{GB}_i)$ is reduced to 0, indicating that GB_i is assigned to negative region will minimize uncertainty loss.
2) When $m(\text{GB}_i) \geq \alpha^*$, $m(\text{GB}_i)$ is elevated to 1, indicating that GB_i is assigned to positive region will minimize uncertainty loss.
3) When $\beta < m(\text{GB}_i) < \alpha^*$, $m(\text{GB}_i)$ is transformed into $[\beta^*, \alpha^*]$, indicating that GB_i is assigned to boundary region will minimize uncertainty loss.

In cases $\beta^* < m(\text{GB}_i) < \alpha^*$, the interval $[\beta^*, \alpha^*]$ represents the GBs in boundary region are described by a great uncertainty.

Obviously, $H\psi_{(\mathbb{X}_{\mathbb{R}}^{\mathbb{J}})}(\text{POS}) = H\psi_{(\mathbb{X}_{\mathbb{R}}^{\mathbb{J}})}(\text{NEG}) = 0$. The total fuzziness of $\psi(\mathbb{X}_{\mathbb{R}}^{\mathbb{J}})$ is computed as follows:

$$\begin{aligned} H_{\psi(\mathbb{X}_{\mathbb{R}}^{\mathbb{J}})} &= H_{\psi(\mathbb{X}_{\mathbb{R}}^{\mathbb{J}})}(\text{BND}) \\ &= T \int_{\beta^*}^{\alpha^*} \bar{\mu}(x)(1 - \bar{\mu}(x))\, d\bar{\mu}(x) \end{aligned} \tag{26}$$

where $T = \frac{4|\{x \in U | \beta^* < \bar{\mu}(x) < \alpha^*\}|}{|U|}$.

Uncertainty measure [38], [43] is a crucial metric in decision system. The calculation of fuzziness does not require expert knowledge, making it more objective. In addition, maintaining fuzziness invariance serves to minimize fuzziness loss. Consequently, based on the fuzziness invariance, an objective function is formulated by combining formulas (19) and (26) to determine the optimal thresholds as follows:

$$\begin{aligned} &\underset{0 \leq \beta^* \leq \alpha^* \leq 1}{\text{argmin}} \left| \bar{H}_{\psi(\mathbb{X}_{\mathbb{R}}^{\mathbb{J}})} - \bar{H}_{\mathbb{X}_{\mathbb{R}}^{\mathbb{J}}} \right| \\ &\text{s.t. } 0 \leq \beta^* \leq 0.5,\ 0.5 \leq \alpha^* \leq 1 \end{aligned} \tag{27}$$

where $H_{\psi(\mathbb{X}_{\mathbb{R}}^{\mathbb{J}})} - H_{\mathbb{X}_{\mathbb{R}}^{\mathbb{J}}}$ is given as follows:

$$H_{\psi(\mathbb{X}_{\mathbb{R}}^{\mathbb{J}})} - H_{\mathbb{X}_{\mathbb{R}}^{\mathbb{J}}} = H_{\psi(\mathbb{X}_{\mathbb{R}}^{\mathbb{J}})}(\text{BND}) - \frac{1}{|U|} \sum_{\text{GB} \in \text{GBs}} \xi(\text{GB}). \tag{28}$$

The process of threshold acquisition is shown in Algorithm S2 in Section S1 of supplementary file. By utilizing the above-mentioned objective function, the optimal thresholds and corresponding three regions can be determined, ensuring minimal fuzziness loss. If alternative thresholds are utilized to develop the 3WD, different regions will be achieved, resulting

in an increased uncertainty loss. Based on the 3WA-SS, 3WC-GBNRS++ is further proposed as follows.

Definition 14: Given a neighborhood decision system NS $= (U, C \cup D, V, f)$, GBs $= \{\text{GB}_1, \text{GB}_2, \ldots, \text{GB}_n\}$ is a GB sapce generated on NS by DBGBC. (β^*, α^*) denotes a threshold pair obtained under 3WA-SS. $R \subseteq C$ and $X \subseteq U$, $\forall \text{GB}_i \in$ GBs, the improved lower approximation, upper approximation, and generation lower approximation of X with respect to R under the 3WA-SS are defined as follows:

$$\underline{\mathbf{G}}(X) = \{x \in U \mid x \in \text{GB}_i, m(\text{GB}_i) \geq \alpha^*\} \tag{29}$$

$$\overline{\mathbf{G}}(X) = \{x \in U \mid x \in \text{GB}_i, m(\text{GB}_i) > \beta^*\} \tag{30}$$

$$\underline{\mathbf{G}'}(X) = \{c_i \mid x \in \text{GB}_i, m(\text{GB}_i) \geq \alpha^*\}. \tag{31}$$

Accordingly, the rules for dividing the three decision regions are defined as

$$\mathbf{POS}_R^{(\beta^*,\alpha^*)}(X) = \underline{\mathbf{G}}(X) \tag{32}$$

$$\mathbf{NEG}_R^{(\beta^*,\alpha^*)}(X) = U - \underline{\mathbf{G}}(X) \tag{33}$$

$$\mathbf{BND}_R^{(\beta^*,\alpha^*)}(X) = \overline{\mathbf{G}}(X) - \underline{\mathbf{G}}(X). \tag{34}$$

To improve the three-way classification accuracy of predicted objects, we employ a linear fitting approach [44] to automatically search the GB neighborhood of predicted objects.

Let $[\boldsymbol{\gamma}^s, \boldsymbol{\gamma Ind}] = \text{sortAscending}(\boldsymbol{\gamma})$. $\boldsymbol{\gamma}$ refers to the set of distance between the predicted object and each GB, as calculated based on Definition 6, that is, $\boldsymbol{\gamma} = (\gamma_1, \ldots, \gamma_N)$. $\boldsymbol{\gamma}^s$ is the ascending order of $\boldsymbol{\gamma}$, and $\boldsymbol{\gamma Ind}$ is the array of indices corresponding to the ascending order of $\boldsymbol{\gamma}$, N denotes the number of GBs. For i from $N-$len and 0 (from the end to beginning), we fit the γ points against their indices to a linear equation with length len

$$\boldsymbol{\gamma}_i^s = a_i \boldsymbol{I}_i + b_i. \tag{35}$$

In the above-mentioned formula, $\boldsymbol{\gamma}_i^s = (\gamma_{i+1}, \gamma_{i+2}, \ldots, \boldsymbol{\gamma}_{i+len})$ and $\boldsymbol{I}_i = (I_{i+1}, I_{i+2}, \ldots, I_{i+len})$. a_i and b_i are two variables solved by achieving a minimum mean square deviation between the fitting function value and the true value. Then, we estimate γ parameter values: $\hat{\gamma}_i = a_i \times \boldsymbol{I}_i + b_i$ and note the difference between the estimated value and the true value for $\Delta\gamma = \gamma_i - \hat{\gamma}_i$. When the first i satisfies the following formulas:

$$\Delta\gamma_i > \text{Local } R \cdot (\mathbf{d}\boldsymbol{\gamma}_i^s) \tag{36}$$

$$\Delta\gamma_i > \text{Global } R \cdot \text{Max}(\mathbf{d}\boldsymbol{\gamma}^s) \tag{37}$$

where γ_i represents the turning point. Select the GBs corresponding to γ values less than γ_i as the nearest neighbors for the predicted objects.

Where $\mathbf{d}\boldsymbol{\gamma}_i^s$ and $\mathbf{d}\boldsymbol{\gamma}^s$ are the difference vectors of $\boldsymbol{\gamma}_i^s$ and $\boldsymbol{\gamma}^s$, respectively. Local R and global R serve as regulatory parameters determining the extent of increment in the turning point's value relative to preceding data points (within the framework of linear fitting movement, "previous" denotes the right side) and the ratio between $\Delta\gamma$ and $\text{Max}(\mathbf{d}\boldsymbol{\gamma}^s)$ for selecting the initial turning point.

As shown in Fig. 2, the actual γ values are represented by black circles, while the predicted γ value before it is currently being linearly fitted is denoted by a red dot. If there is a significant "jump" from the predicted γ value to the actual γ value at position i, the GBs whose γ values are greater than or equal to γ_i are chosen as the neighborhood of predicted object. Algorithm S3 in Section S1 of supplementary file gives the details of choosing the turning point. Based on Algorithm S3, an adaptive GB neighborhood is proposed as follows.

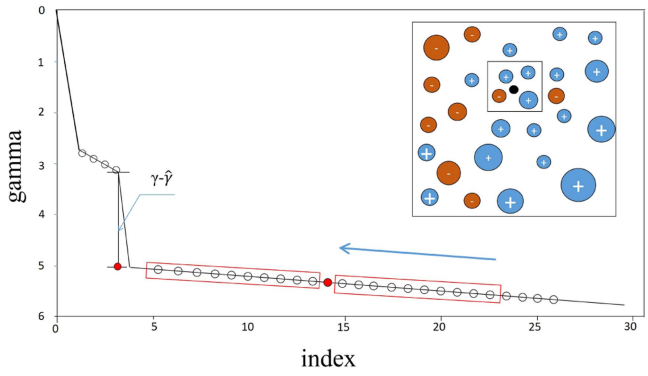

Fig. 2. Diagram to illustrate the adaptive GB neigborhood selection utilizing linear fitting.

Definition 15: Given a neighborhood decision system NS $= (U, C \cup D, V, f)$, GBs $= \{\text{GB}_1, \text{GB}_2, \ldots, \text{GB}_n\}$ is a GB space generated on NS. $R \subseteq C$. x is a predicted object, the distance from x to each GB in GBs are arranged in ascending order, denoted by the set DIS $= \{\gamma_1, \gamma_2, \gamma_3, \ldots, \gamma_n\}$. Utilizing DIS as the raw data, Algorithm S3 is applied to obtain the GB neigborhood $\delta^*_{R(x)}$ of x with respect to R.

According to Definition 3, the average membership of $\delta^*_{R(x)}$ is defined as follows:

$$\nu(x) = \frac{\sum_{\text{GB} \in \delta^*_{R(x)}} l(\text{GB})}{\left|\delta^*_{R(x)}\right|}. \tag{38}$$

The three-way classification rules according to the threshold pair (β^*, α^*) can be expressed as follows:

$$\text{POS}_R^{(\beta^*,\alpha^*)}(X) = \{x \in U \mid \nu(x) \geq \alpha^*\} \tag{39}$$

$$\text{NEG}_R^{(\beta^*,\alpha^*)}(X) = \{x \in U \mid \nu(x) \leq \beta^*\} \tag{40}$$

$$\text{BND}_R^{(\beta^*,\alpha^*)}(X) = \{x \in U \mid \beta^* < \nu(x) < \alpha^*\}. \tag{41}$$

The details of three-way classification based on 3WC-GBNRS++ is shown in Algorithm 2. The time complexity of Algorithm 2 is $O(N)$, which is explained as follows: calculating the distance for each GB typically involves all GBs, so the time complexity for this step is $O(N)$. Based on the analysis of Algorithm S3, computing the adaptive GB neighborhood of x_{test} takes $O(N)$ time. The calculation of $\nu(x_{\text{test}})$ involves the number of labels in the neighborhood of x_{test}, which does not exceed N. Therefore, this step has a time complexity of $O(N)$. The predicted objects with $\nu(x_{\text{test}})$ exceeding the threshold α^* is designated as the positive label; the predicted objects with $\nu(x_{\text{test}})$ below the threshold β^* is designated as the negative

TABLE I
INFORMATION OF EXPERIMENTAL DATASETS

ID	Datasets	Characteristics	Instances	Attributes	Source
D_1	HCV	Categorical	596	10	[45]
D_2	Breast-cancer	Integer	699	9	[45]
D_3	Energy effciency	Integer, real	768	8	[45]
D_4	Endgame	Categorical	958	9	[45]
D_5	Heart	Real	1025	13	[46]
D_6	Car	Categorical	1728	6	[47]
D_7	Spambase	Integer, real	4601	57	[45]
D_8	Banana	Real	5300	2	[47]
D_9	Elect	Real	10000	12	[45]
D_{10}	Penbased	Integer	10992	16	[45]
D_{11}	Dry bean	Integer, real	13611	16	[45]
D_{12}	HTRU_2	Real	17898	8	[45]

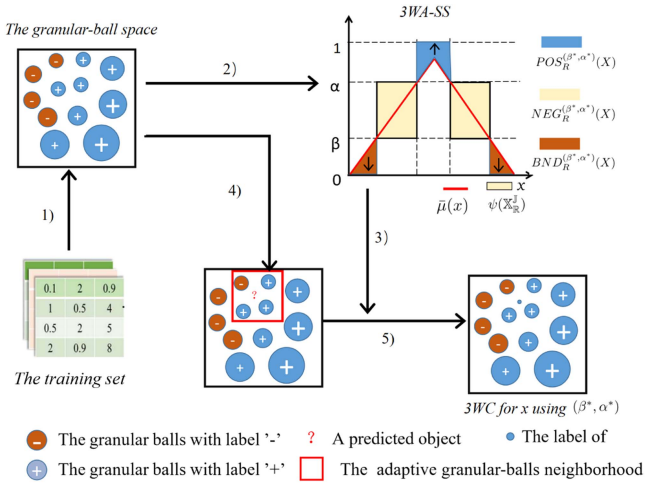

Fig. 3. Construction process of 3WC-GBNRS++ from the perspective of uncertainty.

label; the predicted objects with $\nu(x_{\text{test}})$ falls between β^* and α^* is regarded as the delayed label.

Fig. 3 illustrates the construction process of 3WC-GBNRS++. Step 1) the original dataset is transformed into the density-based GBs by DBGBC; Step 2)–3) the thresholds (β^*, α^*) are determined by minimizing fuzziness loss between $\mathbb{X}_{\mathbb{R}}^{\mathbb{J}}$ and $\psi(\mathbb{X}_{\mathbb{R}}^{\mathbb{J}})$ based on the objective function. That is, 3WA-SS is introduced to provide thresholds for GBNRS++. Specially, the actual uncertainty of each granular space is captured through $\mathbb{X}_{\mathbb{R}}^{\mathbb{J}}$. Step 4) The adaptive GB neighborhood of a predicted object x_{test} is obtained; Step 5) x_{test} is classified according to (β^*, α^*).

Compared to 3WD-NRS, 3WD-GBNRS++ utilizes GBs instead of individual sample points as inputs, which enhances the classification efficiency. Moreover, the label of a GB is determined by the majority label, which eliminates the impact of noise data in each GB and improve the robustness of 3WD-GBNRS++.

V. EXPERIMENT

In this section, we present the experimental setup, including validation procedures, evaluation metrics, comparison methods, and hyperparameter configurations. Subsequently, we conduct an ablation study to demonstrate the effectiveness of our proposed approach. Finally, we provide a comprehensive overview of the performance of 3WC-GBNRS++ in terms of efficiency stability, and robustness. The experiments are focused on two key research aspects as follows.

1) Comparison to GBNRS++, 3WC-GBNRS++ results in a less fuzziness loss. This is demonstrated by quantitative results obtained from experiments.
2) 3WC-GBNRS++ outperforms the GBs-based classifiers and conventional classifier algorithms, including KNN, SVM, CART, GBNRS, GBKNN, ACCGBNRS, etc., in terms of comprehensive performance. This conclusion is drawn from measurements using specific evaluation criteria in experiments.

All experiments are operated on a system with an Intel i5-4210 M CPU (clock speed of 2.60-GHz), 8.0 GB of DDR3 running memory, Windows 10, 64-bit OS and the programming software is Python 3.9.7. Experiments are performed based on 12 UCI datasets, which are shown in Table I. Remarkably, the unstructured datasets involved have been converted into structured numerical datasets by the providers. The incomplete samples in the dataset were removed. To mitigate the influence of dimensions on the classifier's learning process, all datasets utilized have been normalized.

Algorithm 2: Three-way Classification Based on 3WD-GBNRS++.

Input: $DBGB\_list$, $\delta_R^*(x_{\text{test}})$ and (α^*, β^*).
Output: The class label $label$ of predicted object x_{test}.

Function *Main*($DBGB\_list$, $\delta_R^*(x_{test})$, α^*, β^*)**:**
  $region = \{\}$;
  for GB *in* $DBGB\_list$ **do**
    Calculate the distance from x_{test} to GB;
  end
  Calculate the adaptive granular-ball neighborhood of x_{test};
  Calculate $\nu(x_{test}) = \frac{\sum_{GB \in \delta_R^*(x_{test})} l(GB)}{|\delta_R^*(x_{test})|}$;
  if $\nu(x_{test}) \geq \alpha^*$ **then**
    $label \leftarrow +$;
  end
  else if $\nu(x_{test}) \leq \beta^*$ **then**
    $label \leftarrow -$;
  end
  else
    $label \leftarrow *$;
  end
  return $label$;
return

A. General Settings

Validation procedures and evaluation metrics: To mitigate the potential false performance resulting from overfitting, we utilize the ten-fold cross-validation technique in each section of

Section V to accurately assess the true generalizability of our proposed method.

For the first experiment, it is essential to validate the efficacy of the 3WC-GBNRS++. Compared to GBNRS, 3WC-GBNRS++ is constructed from the perspective of minimizing fuzziness loss, therefore fuzziness loss is chosen as the evaluation metric for this experiment. The formula (28) is used to calculate the total fuzziness loss for GBNRS and 3WC-GBNRS++.

In the second experiment, the performance of 3WC-GBNRS++ is validated, including accuracy, time cost, robustness and stability. In terms of effectiveness, in addition to accuracy, four common machine learning metrics, that is, Accuracy, Precision, Recall, and F1 score ($F1$) are also calculated for further assessment. The larger the values of these three metrics, the better the classification performance. Herein, $F1$ represents the harmonic mean between Precision and Recall. Accuracy refers to two variables, R_{test} and U_{test}, are defined to the ratio of the number of correctly predicted test samples to the number of total test samples. Precision indicates the proportion of elements predicted as positive that are actually correct, while Recall indicates the proportion of elements that are actually positive and correctly identified. Assuming the total number of correctly predicted positive elements is tp, the total number of correctly predicted negative elements is tn, the total number of false positives is fp, and the total number of false negatives is fn, the formulas for, Accuracy, Precision, Recall, and $F1$ are as follows:

$$\text{Accuracy} = \frac{R_{\text{test}}}{U_{\text{test}}} \tag{42}$$

$$\text{Precision} = \frac{tp}{tp + fp} \tag{43}$$

$$\text{Recall} = \frac{tp}{tp + fn} \tag{44}$$

$$\text{F1} = \frac{2 \times \text{Precision} \times \text{Recall}}{\text{Precision} + \text{Recall}}. \tag{45}$$

Moreover, we utilize the Wilcoxon rank-sum test to determine whether there are significant differences between the compared classifiers. In addition, the performance of the method is further validated through the time cost, as well as the antinoise capability and stability. Relevant evaluation criteria will be mentioned in the corresponding experimental sections.

Comparison methods and hyperparameter settings: 3WC-GBNRS++ is compared with three state-of-the-art GB-based classifiers and four classic machine learning classifiers. The descriptions of these classifiers and their hyperparameter settings are as follows.

1) *KNN:* Set k to 1, 3, 5, 7, 9, 11, 13, and 15 and select the appropriate k value as the final result.
2) *ML-KNN:* It incorporates probabilistic reasoning to estimate the likelihood of label existence.
3) *NC:* It is a neighbor-counting-based classification algorithm. It divides elements into several classes based on their similarity, with higher similarity observed within the same class and lower similarity observed between different classes.

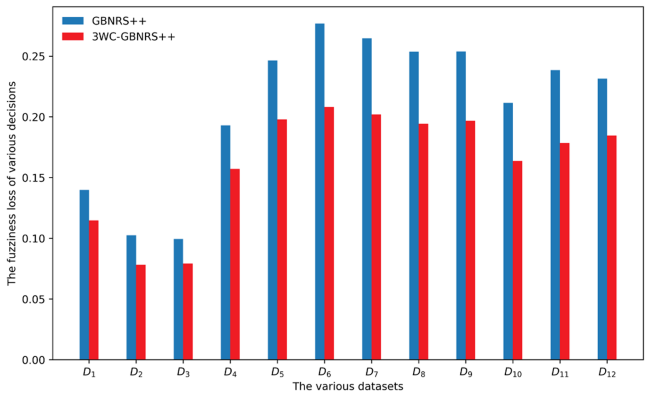

Fig. 4. Fuzziness loss between GBNRS++ and 3WC-GBNRS++ on various datasets.

4) *CART:* All hyperparameters of CART are consistent with the default parameters in scikit-learn.
5) *SVM:* Uses the radial basis function as the kernel function, with the hyperparameter set to the reciprocal of the number of features in the dataset.
6) *GBNRS [32]:* It is an original GB-based NRS. The setting of k for k-NN in ORI-GBNRS is the default value of 1.
7) *GBKNN [25]:* It is an original GB-based KNN algorithm. The value of k for this algorithm is determined by the linear fitting algorithm proposed in this article.
8) *GBKNN++ [48]:* It is an improved GB-based KNN algorithm based on GBG++ method. The nearest GB is determined according to the harmonic distance, that is, the k value is set to 1.
9) *ACC-GBKNN [26]:* In this classifier, the K-means method in ACC-GBCKNN classifier is replaced by k-division. The setting of k for k-NN is the default value of 1.

B. GBNRS++ Versus 3WC-GBNRS++(RP. 1)

Fig. 4 illustrates the fuzziness loss of GBNRS++ and 3WC-GBNRS++ in classification on 12 datasets. It is obviously that 3WC-GBNRS++ effectively reduces the fuzziness loss during the actual classification process compared to GBNRS++. Consequently, 3WC-GBNRS++ maintains the advantages of GBNRS++ while avoiding additional fuzziness loss, because the construction principle of 3WC-GBNRS++ is based on minimum fuzziness loss. Therefore, 3WC-GBNRS++ maintains less fuzziness loss than GBNRS++, as demonstrated by quantitative results obtained from experiments.

C. 3WC-GBNRS++ Versus Other Classifier (RP. 2)

Effectiveness: The comparison experiment includes nine different classification algorithms, including KNN, SVM, CART, GBNRS, GBKNN, GBKNN++, and ACC-GBKNN, etc. Table II presents four evaluation metrics, namely Accuracy, Precision, Recall, and $F1$. Subsequently, statistical analysis is performed on the results, including the Friedman test, Wilkerson rank-sum test, and mean ranking analysis. Win/Loss represents the

TABLE II
STATISTICAL ANALYSIS OF VARIOUS ALGORITHMS

No.	Metrics	KNN	ML-KNN	NC	CART	SVM	GBNRS	GBKNN	GBKNN++	ACC-GBKNN	3WC-GBNRS++
D_1	AC	0.9548	0.9548	0.9429	0.98	0.9565	0.9056	0.9362	0.9265	0.9349	0.9680
	$F1$	0.9754	0.9754	0.9685	0.9888	0.9763	0.9427	0.9650	0.6919	0.7963	0.9833
	Re	0.9571	0.9944	0.9590	0.9834	0.9575	0.9655	0.9501	0.9944	0.9739	0.9812
	P	0.9944	0.9576	0.9793	0.9944	0.9963	0.9302	0.9812	0.9298	0.9553	0.9863
D_2	AC	0.9386	0.9384	0.9277	0.7854	0.9407	0.9471	0.9360	0.9346	0.9411	0.9552
	$F1$	0.9328	0.9254	0.9245	0.7575	0.9294	0.9316	0.9173	0.9340	0.9408	0.9643
	Re	0.9265	0.9067	0.9089	0.7166	0.9600	0.9911	0.9826	0.9407	0.9409	0.9881
	P	0.9392	0.9668	0.9530	0.8409	0.9203	0.8974	0.8835	0.9325	0.9421	0.9424
D_3	AC	0.9095	0.8679	0.9289	0.9724	0.9185	0.9094	0.9149	0.9208	0.9039	0.9561
	$F1$	0.9214	0.8621	0.9463	0.9729	0.9339	0.9212	0.9106	0.9168	0.9026	0.9531
	Re	0.8932	0.8485	0.9184	0.9616	0.9178	0.9191	0.9368	0.8848	0.9121	0.9203
	P	0.9515	0.9176	1.0000	0.9909	0.9758	0.9485	0.9000	0.9253	0.8879	0.9966
D_4	AC	0.7676	0.8176	0.5691	0.8072	0.8457	0.6954	0.7038	0.6817	0.7005	0.9812
	$F1$	0.8220	0.8754	0.6202	0.8126	0.8814	0.7853	0.7891	0.6565	0.6726	0.9901
	Re	0.8212	0.9507	0.7076	0.9154	0.8891	0.7282	0.7395	0.7222	0.7556	0.9812
	P	0.8228	0.8171	0.5821	0.7732	0.8802	0.8613	0.8501	0.7780	0.7800	1.0000
D_5	AC	0.8177	0.7878	0.7910	0.7113	0.8211	0.7944	0.7880	0.7980	0.7615	0.8333
	$F1$	0.8309	0.7968	0.8094	0.7018	0.8409	0.8009	0.7979	0.7949	0.7560	0.8430
	Re	0.8166	0.7838	0.7952	0.7237	0.8172	0.8294	0.8167	0.8040	0.7915	0.8560
	P	0.8456	0.8170	0.8331	0.7081	0.8765	0.7838	0.7897	0.8270	0.7836	0.8400
D_6	AC	0.9554	0.9433	0.8512	0.8917	0.9635	0.9201	0.9305	0.9091	0.9144	0.9754
	$F1$	0.9677	0.9597	0.8831	0.9298	0.9739	0.9447	0.9523	0.8945	0.8940	0.9843
	Re	0.9804	0.9595	0.9611	0.9036	0.9793	0.9269	0.9325	0.9165	0.9529	0.976
	P	0.9554	0.9626	0.8215	0.9661	0.9694	0.9653	0.9744	0.9538	0.9294	0.9933
D_7	AC	0.7843	0.7753	0.8059	0.7957	0.8698	0.7544	0.7929	0.8647	0.8597	0.9021
	$F1$	0.7120	0.7303	0.7464	0.7726	0.8233	0.6491	0.6894	0.8593	0.8544	0.8288
	Re	0.6976	0.7966	0.7911	0.7583	0.8715	0.7926	0.8361	0.8397	0.8320	0.9417
	P	0.7269	0.7294	0.7675	0.8313	0.8175	0.6240	0.6584	0.8272	0.8243	0.7517
D_8	AC	0.8079	0.8056	0.5096	0.7346	0.8736	0.7841	0.8962	0.8826	0.8688	0.9678
	$F1$	0.7896	0.7834	0.3851	0.7304	0.8576	0.7739	0.8793	0.8810	0.8678	0.9612
	Re	0.7951	0.7677	0.3990	0.71	0.8872	0.7642	0.9183	0.8542	0.8727	0.9747
	P	0.7842	0.8213	0.4852	0.7774	0.8410	0.8056	0.8439	0.8805	0.8412	0.9484
D_9	AC	0.9127	0.9235	0.8686	0.9998	0.9747	0.8884	0.8969	0.8607	0.8463	0.9856
	$F1$	0.8686	0.8930	0.8339	0.9997	0.9657	0.8406	0.8382	0.8507	0.8367	0.9642
	Re	0.9372	0.8848	0.7886	0.9997	0.9672	0.8747	0.9538	0.8312	0.8351	0.9765
	P	0.8094	0.9070	0.9006	0.9997	0.9663	0.8141	0.7550	0.7941	0.7633	0.9539
D_{10}	AC	0.9773	0.9774	0.7225	0.8857	0.9847	0.9821	0.9660	0.9953	0.9944	0.9998
	$F1$	0.8646	0.8783	0.4078	0.6918	0.9002	0.8864	0.7775	0.9873	0.9849	0.9979
	Re	0.9483	0.8904	0.3199	0.7255	0.9784	0.9585	0.9522	0.9799	0.9746	1.0000
	P	0.8491	0.9241	0.8386	0.7948	0.8763	0.8746	0.7247	0.9748	0.9715	0.9958
D_{11}	AC	0.9759	0.9750	0.8548	0.9456	0.9804	0.9672	0.9742	0.9439	0.9450	0.9881
	$F1$	0.9205	0.9154	0.7653	0.802	0.9326	0.8922	0.9149	0.9066	0.9033	0.9602
	Re	0.9140	0.9113	0.7072	0.8505	0.9494	0.9013	0.9184	0.9032	0.8884	0.9616
	P	0.9270	0.9316	0.9581	0.823	0.9221	0.9004	0.9226	0.8175	0.8096	0.9624
D_{12}	AC	0.9620	0.9771	0.9416	0.6357	0.9687	0.9391	0.9698	0.9752	0.9735	0.9883
	$F1$	0.7588	0.8666	0.7244	0.3067	0.7743	0.7290	0.7667	0.9227	0.9191	0.9245
	Re	0.7377	0.8152	0.6746	0.4206	0.9428	0.8809	0.8452	0.8279	0.8402	0.9690
	P	0.7811	0.9278	0.8029	0.6397	0.7787	0.7835	0.7720	0.8951	0.8698	0.8852
Statistics	$win/loss$	45/3	45/3	45/3	36/12	42/6	47/1	47/1	44/4	46/2	397/35
	$p-vlaue$	1.5806E-07	3.5988E-07	3.1589E-10	6.5908E-06	2.7852E-04	1.1918E-08	6.0006E-08	1.7453E-07	7.5117E-08	
	$rank$	**5.4688(3)**	5.3854	3.5625	4.4479	**7.4583(2)**	4.4583	4.9792	5.2604	4.7083	**9.2708(1)**

win-loss ratio following pairwise comparisons between 3WC-GBNRS++ and the comparison algorithms. $p-$value reflects the difference between 3WC-GBNRS++ and the comparison methods. If $p-$value < 0.05, it indicates a significant difference between 3WC-GBNRS++ and the comparison algorithms; otherwise, there is no statistical difference. Rank represents the average ranking. A higher rank value indicates a more effective algorithm. As shown in Table II, in terms of Win/Loss, 3WC-GBNRS++ wins 397 times out of 432 total comparison times against other algorithms. In terms of $p-$value, 3WC-GBNRS++ shows significant differences with the comparison algorithms. Regarding rank, 3WD-GBNRS++ obtains the highest overall score, followed by SVM and traditional KNN.

The superior performance of 3WC-GBNRS++ in terms of effectiveness can be attributed to the following reasons.

1) Compared to the five traditional classifiers, 3WC-GBNRS++ inherits the advantages of GBs-based classifiers. That is, GBs are more suitable for describing datasets with spherical distributions and exhibit robustness to noisy data.
2) Compared to the four GBs-based classifiers, the proposed DBGBC is utilized to generate GBs in 3WC-GBNRS++, resulting in granulation results with higher quality.
3) The idea of 3WD is helpful to uncertainty, which improves the classification performance to a great extent.
4) 3WC-GBNRS++ selects an appropriate GBs neighborhood to classify the test points, which is more objective in a data-driven method.

Efficiency: Table III presents the time required for 3WC-GBNRS++ and comparison methods on each dataset. With the increase in dataset size, the time required for classification by KNN and ML-KNN significantly increases. From Table II, it is evident that the comprehensive score of NC is much lower than that of other algorithms. In addition, we conducted a statistical analysis of Table III. When the threshold of $p-$value is 0.1, 3WC-GBNRS++ shows significant differences from KNN,

TABLE III
REQUIRED TIME OF VARIOUS ALGORITHMS

No.	KNN	ML-KNN	NC	CART	SVM	GBNRS	GBKNN	GBKNN++	ACC-GBKNN	3WC-GBNRS++
D_1	0.6345	0.4833	0.0017	0.0493	0.0130	0.0856	0.0995	0.0815	0.1680	0.1069
D_2	0.4290	0.9948	0.0027	0.0463	0.0061	0.0258	0.0369	0.0409	0.1346	0.0585
D_3	0.7792	1.1836	0.0018	0.0497	0.0092	0.0432	0.0697	0.0415	0.1457	0.2244
D_4	1.5192	2.0369	0.0021	0.0491	0.0358	0.3132	0.2919	0.1553	0.6382	0.3737
D_5	0.1394	0.4053	0.0028	0.047	0.0092	0.0299	0.0399	0.0406	0.1598	0.0415
D_6	3.9982	5.7310	0.0018	0.0553	0.0419	0.2809	0.3018	0.1813	0.3784	0.3044
D_7	27.7183	82.3622	0.0042	0.2259	0.4902	4.2622	3.9653	1.3210	3.9071	5.7495
D_8	38.1918	137.8585	0.0034	0.0724	0.5186	3.8877	4.0635	0.7590	2.6914	3.8152
D_9	154.1780	190.8764	0.0031	0.1097	1.1476	26.7855	25.0774	2.9655	9.6169	22.4422
D_{10}	153.1094	758.7321	0.0093	0.1092	0.5219	3.8038	5.0175	0.7873	1.6312	20.6239
D_{11}	280.7096	705.0898	0.0047	0.8426	0.9366	12.8698	9.3752	1.3612	5.9831	10.0290
D_{12}	367.3679	2197.1564	0.0419	0.4712	1.2582	28.0087	25.2570	2.5493	10.0849	24.0669
$p-$ vlaue	**0.0496**	**0.0327**	**4.1460E-05**	**0.0153**	**0.0433**	0.6861	0.6861	0.1124	0.8174	
rank	2.1667	**1.25(10)**	**10(1)**	7.7500	8.5000	5.0833	4.9167	6.8333	4.5000	**4(8)**

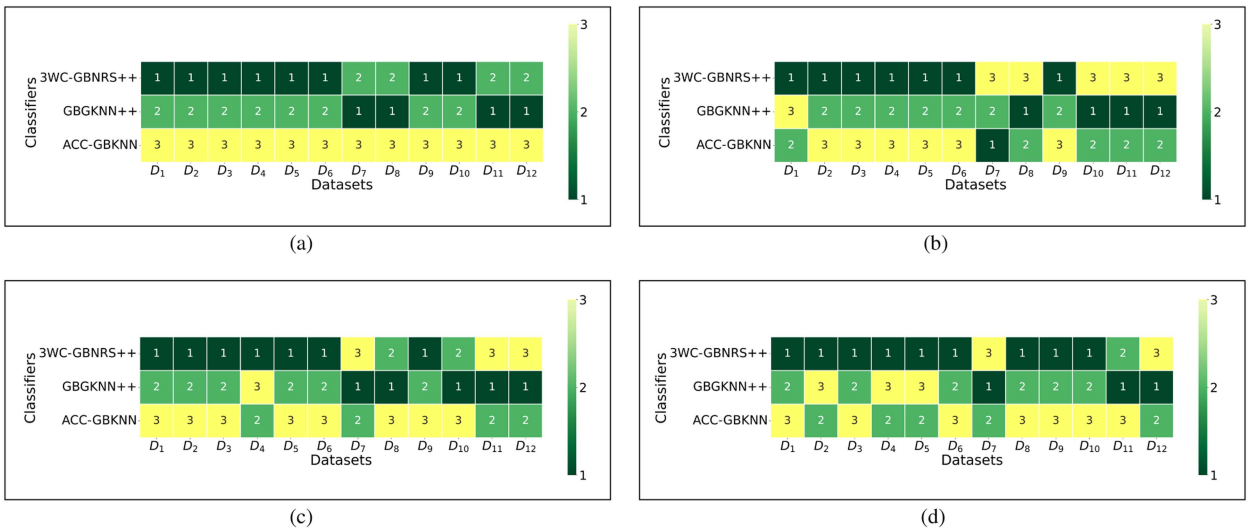

Fig. 5. Comparison on ranking of test Accuracy under each noise rate. (a) Noise rate: 10%. (b) Noise rate: 20%. (c) Noise rate: 30%. (d) Noise rate: 40%.

ML-KNN, NC, CART, and SVM. From the perspective of rankings, the time consumed by 3WC-GBNRS++ ranks 8th among all the algorithms, while the other GB-based methods, namely GBKNN++, GBNRS, GBKNN, ACC-GBKNN, rank from 4th to 7th. This implies that the time required by 3WC-GBNRS++ is not significantly different from that of other GB-based methods. Although the time consumption of 3WC-GBNRS++ is much higher than that of NC (the 1st ranked), much lower than that of ML-KNN in the last place.

Due to the introduction of DBGBC, 3WC-GBNRS++ incurs slightly more time compared to the other GBs-based methods. However, this increase of time cost is entirely acceptable. Overall, 3WC-GBNRS++ provides a classification solution with relatively low time complexity.

Robustness: To verify the robustness of 3WC-GBNRS++, we manually construct the noise proportions of 10%, 20%, 30%, and 40% on each dataset. From literatures [25], [48], it is obviously that the robustness of GBs-based classifiers outperforms that of conventional classifiers. Therefore, for this evaluation, we only selected two state-of-the-art GBs-based classifiers, ACC-GBKNN and GBKNN++, as the comparison methods. The specific steps involved are as follows. 1) Random samples are chosen on each dataset, and the labels of these samples are changed. 2) Ten-fold cross-validation is performed on datasets with different noise ratios to measure the robustness performance of these classifiers based on test accuracy. From Fig. 5, the results are visualized using a heat map, indicating the ranking of test accuracy for classifiers on any dataset under any label noise ratio. For instance, on the HCV dataset with a label noise ratio of 10%, 3WC-GBNRS++ achieves the highest test accuracy, marked as 1 in Fig. 5(a). As illustrated in Fig. 5, 3WC-GBNRS++ ranks first on most datasets, outperforming GBKNN++ and ACC-GBKNN in terms of test accuracy for the majority of datasets with label noise ratios of 10%, 20%, 30%, and 40%. The main reason for the outstanding noise robustness of 3WC-GBNRS++ is that 3WC-GBNRS++ configured with DBGBC naturally mitigates the impact of noisy samples, since the label of a GB is determined by the majority of samples,

Stability: To verify the stability of multiple classification results of 3WC-GBNRS++ on the same dataset, we selected ACC-GBKNN and GBKNN++, as the comparison methods.

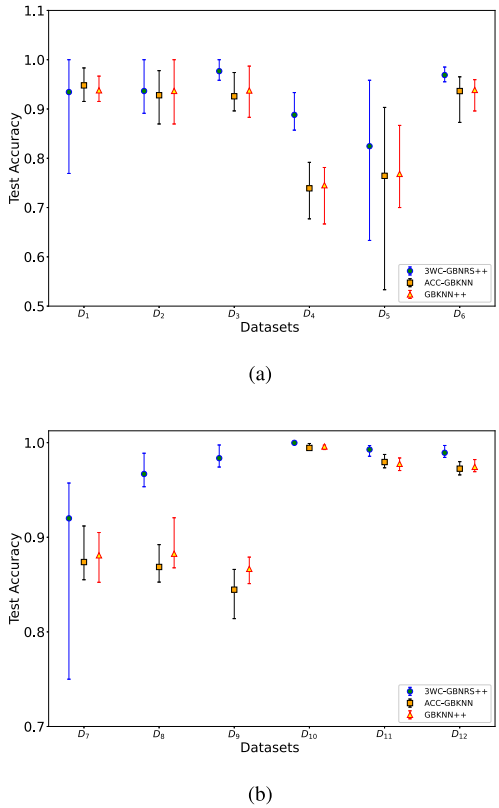

Fig. 6. Comparison on stability of GB-based classifiers. (a) Stability on test Accuracy on first group datasets. (b) Stability on test Accuracy on second group datasets.

Each classifier performs an additional nine rounds of ten-fold cross-validation. The mean, minimum, and maximum of the test accuracy are jointly considered. Error bars are used to visualize experimental results, where the central line, top line, and bottom line of the error bar represent the average, maximum, and minimum values of the test accuracy from ten rounds of ten-fold cross-validation, respectively. Notably, the data partition remains unchanged in this section.

As shown in Fig. 6, it is worth noting that the stability of the classification results of 3WC-GBNRS++ and ACC-GBKNN is poor when executed repeatedly on the same dataset, while GBKNN++ demonstrates better stability in its classification results on the same dataset. The reason is that 3WC-GBNRS++ and ACC-GBKNN rely on random centers during the process of splitting GBs, and GBKNN++ does not require random parameters when given a purity threshold. In summary, there is still room for improvement in the stability of 3WC-GBNRS++.

VI. Conclusion

To enhance the efficiency and precision of the 3WDNRS framework, this article introduced a three-way classifier with GBNRS++, namely 3WC-GBNRS++, which incorporated the 3WD approach based on minimum fuzziness loss. The experimental results demonstrated that 3WC-GBNRS++ effectively reduces the fuzziness loss during the classification process compared to GBNRS++. 3WC-GBNRS++ almost outperformed other comparison methods in terms of effectiveness and robustness, including four state-of-the-art GBs-based classifiers and five classical machine learning classifiers on 12 public benchmark datasets. Therefore, our works provided a solid foundation for future work in developing 3WD theory with more robust and generality. Nevertheless, our work remained exploratory and possesses certain limitations as follows.

1) Compared with the current GB-based classifier, GB generation in 3WC-GBNRS++ is more time-consuming, which needs to be further improved.
2) Lack of a multilevel framework of sequential 3WC-GBNRS++ and its optimal GB space selection method for decision-making.

The focus of our future work will be on the following three aspects.

1) An incremental learning based on 3WC-GBNRS++ will be designed for online feature selection by considering the updating mechanism of GBs.
2) To further improve the efficiency of GB generation in 3WC-GBNRS++, we will draw on the works of GB-based unsupervised learning by utilizing the distributional characteristics. Moreover, as two guidelines of justifiable granularity, coverage, and specificity metrics provide a broader assessment of granulation quality, we will take coverage and specificity metrics as the optimization factor to construct the optimal GB space selection mechanism.
3) Autoencoder network is an efficient representation learning method. We will introduce 3WC-GBNRS++ with optimal GB space selection into the autoencoder network. The research objectives include optimizing the input space, granulating the network structure, and balancing the misclassification cost and the time cost in autoencoder-based classifications.

References

[1] Y. Y. Yao, "The superiority of three-way decisions in probabilistic rough set models," *Inf. Sci.*, vol. 181, no. 6, pp. 1080–1096, 2011.
[2] Y. Y. Yao, "Three-way granular computing, rough sets, and formal concept analysis," *Int. J. Approx. Reasoning*, vol. 116, pp. 106–125, 2020.
[3] J. Deng, J. M. Zhan, E. Herrera-Viedma, and F. Herrera, "Regret theory-based three-way decision method on incomplete multi-scale decision information systems with interval fuzzy numbers," *IEEE Trans. Fuzzy Syst.*, vol. 31, no. 3, pp. 982–996, Mar. 2023.
[4] P. Witold and B. Andrzej, "An optimization of allocation of information granularity in the interpretation of data structures: Toward granular fuzzy clustering," *IEEE Trans. Syst., Man, Cybern., Part B*, vol. 42, no. 3, pp. 582–590, Jun. 2012.
[5] G. Y. Wang, J. Yang, and J. Xu, "Granular computing: From granularity optimization to multi-granularity joint problem solving," *Granular Comput.*, vol. 2, pp. 105–120, 2017.
[6] G. Y. Wang, C. L. Xu, and D. Y. Li, "Generic normal cloud model," *Inf. Sci.*, vol. 280, pp. 1–15, 2014.
[7] D. D. Guo, C. M. Jiang, and P. Wu, "Three-way decision based on confidence level change in rough set," *Int. J. Approx. Reasoning*, vol. 143, pp. 57–77, 2022.
[8] G. M. Lang, J. F. Luo, and Y. Y. Yao, "Three-way conflict analysis: A unification of models based on rough sets and formal concept analysis," *Knowl.-Based Syst.*, vol. 194, pp. 545–556, 2020.
[9] Y. Yao and J. Yang, "Granular rough sets and granular shadowed sets: Three-way approximations in Pawlak approximation spaces," *Int. J. Approx. Reasoning*, vol. 142, pp. 231–247, 2022.
[10] T. X. Wang, H. X. Li, Y. H. Qian, B. Huang, and X. Z. Zhou, "A regret-based three-way decision model under interval type-2 fuzzy environment," *IEEE Trans. Fuzzy Syst.*, vol. 30, no. 1, pp. 175–189, Jan. 2022.

[11] A. Savchenko and L. Savchenko, "Three-way classification for sequences of observations," *Inf. Sci.*, vol. 648, 2023, Art. no. 119540.
[12] Y. N. Lu, W. W. Li, H. X. Li, and X. Y. Jia, "Predicting label distribution from tie-allowed multi-label ranking," *IEEE Trans. Pattern Anal. Mach. Intell.*, vol. 45, no. 12, pp. 15364–15379, Dec. 2023.
[13] P. X. Wang, H. Shi, X. B. Yang, and J. S. Mi, "Three-way k-means: Integrating k-means and three-way decision," *Int. J. Mach. Learn. Cybern.*, vol. 10, pp. 2767–2777, 2019.
[14] H. X. Li, L. B. Zhang, X. Z. Zhou, and B. Huang, "Cost-sensitive sequential three-way decision modeling using a deep neural network," *Int. J. Approx. Reasoning*, vol. 85, no. C., pp. 68–78, 2017.
[15] J. M. Zhan, J. Wang, W. P. Ding, and Y. Y. Yao, "Three-way behavioral decision making with hesitant fuzzy information systems: Survey and challenges," *IEEE/CAA J. Automatica Sinica*, vol. 10, no. 2, pp. 330–350, Feb. 2023.
[16] Q. H. Hu, D. R. Yu, J. F. Liu, and C. X. Wu, "Neighborhood rough set based heterogeneous feature subset selection," *Inf. Sci.*, vol. 178, no. 18, pp. 3577–3594, 2008.
[17] W. W. Li, Z. Q. Huang, X. Y. Jia, and X. Y. Cai, "Neighborhood based decision-theoretic rough set models," *Int. J. Approx. Reasoning*, vol. 69, pp. 1–17, 2016.
[18] Q. Q. Huang, Y. Y. Huang, T. R. Li, and X. Yang, "Dynamic three-way neighborhood decision model for multi-dimensional variation of incomplete hybrid data," *Inf. Sci.*, vol. 597, pp. 358–391, 2022.
[19] J. Ye, J. M. Zhan, W. P. Ding, and H. Fujita, "A novel three-way decision approach in decision information systems," *Inf. Sci.*, vol. 584, pp. 1–30, 2022.
[20] X. Yang, T. R. Li, D. Liu, and H. Fujita, "A multilevel neighborhood sequential decision approach of three-way granular computing," *Inf. Sci.*, vol. 538, pp. 119–141, 2020.
[21] X. L. Chu et al., "Neighborhood rough set-based three-way clustering considering attribute correlations: An approach to classification of potential gout groups," *Inf. Sci.*, vol. 535, pp. 28–41, 2020.
[22] S. Y. Xia et al., "Complete random forest based class noise filtering learning for improving the generalizability of classifiers," *IEEE Trans. Knowl. Data Eng.*, vol. 31, no. 11, pp. 2063–2078, Nov. 2019.
[23] S. Y. Xia et al., "An efficient and accurate rough set for feature selection, classification, and knowledge representation," *IEEE Trans. Knowl. Data Eng.*, vol. 35, no. 8, pp. 7724–7735, Aug. 2023.
[24] D. D. Cheng, Y. Li, S. Y. Xia, G. Y. Wang, J. L. Huang, and S. L. Zhang, "A fast granular-ball-based density peaks clustering algorithm for large-scale data," *IEEE Trans. Neural Netw. Learn. Syst.*, early access, Aug. 11, 2023, doi: 10.1109/TNNLS.2023.3300916.
[25] S. Y. Xia, Y. S. Liu, X. Ding, G. Y. Wang, H. Yu, and Y. G. Luo, "Granular ball computing classifiers for efficient, scalable and robust learning," *Inf. Sci.*, vol. 483, pp. 136–152, 2019.
[26] S. Y. Xia, X. C. Dai, G. Y. Wang, X. B. Gao, and E. Giem, "An efficient and adaptive granular-ball generation method in classification problem," *IEEE Trans. Neural Netw. Learn. Syst.*, vol. 35, no. 4, pp. 5319–5331, Apr. 2024.
[27] S. Y. Xia et al., "Graph-based representation for image based on granular-ball," 2023, *arXiv:2303.02388*.
[28] S. Y. Xia, J. C. Chen, B. Hou, and G. Y. Wang, "Granular-ball optimization algorithm," 2023, *arXiv:2303.12807*.
[29] S. Y. Xia, X. Y. Lian, and Y. B. Shao, "Fuzzy granular-ball computing framework and its implementation in svm," 2022, *arXiv:2210.11675*.
[30] Y. Chen, P. X. Wang, X. B. Yang, J. S. Mi, and D. Liu, "Granular ball guided selector for attribute reduction," *Knowl.-Based Syst.*, vol. 229, 2021, Art. no. 107326.
[31] Q. H. Zhang, C. Y. W. S. Y. Xia, F. Zhao, M. Gao, Y. L. Cheng, and G. Y. Wang, "Incremental learning based on granular ball rough sets for classification in dynamic mixed-type decision system," *IEEE Trans. Knowl. Data Eng.*, vol. 35, no. 9, pp. 9319–9332, Sep. 2023.
[32] S. Y. Xia, H. Zhang, W. H. Li, G. Y. Wang, E. Giem, and Z. Z. Chen, "GBNRS: A novel rough set algorithm for fast adaptive attribute reduction in classification," *IEEE Trans. Knowl. Data Eng.*, vol. 34, no. 3, pp. 1231–1242, Mar. 2022.
[33] D. Dubois and H. Prade, "Rough fuzzy sets and fuzzy rough sets," *Int. J. Gen. Syst.*, vol. 17, no. 2/3, pp. 191–209, 1990.
[34] K. Z. J. M. Zhan and W. Z. Wu, "Novel fuzzy rough set models and corresponding applications to multi-criteria decision-making," *Fuzzy Sets Syst.*, vol. 383, pp. 92–126, 2020.
[35] J. Ye, J. M. Zhan, W. P. Ding, and H. Fujita, "A novel fuzzy rough set model with fuzzy neighborhood operators," *Inf. Sci.*, vol. 544, pp. 266–297, 2021.
[36] J. M. Zhan, X. H. Zhang, and Y. Y. Yao, "Covering based multigranulation fuzzy rough sets and corresponding applications," *Artif. Intell. Rev.*, vol. 53, pp. 1093–1126, 2020.
[37] A. Deluca and S. Termini, "A definition of non-probabilistic entropy in setting of fuzzy set theory," *Inf. Control*, vol. 20, no. 4, pp. 301–312, 1971.
[38] Q. H. Zhang, Y. Xiao, and G. Y. Wang, "A new method for measuring fuzziness of vague set (or intuitionistic fuzzy set)," *J. Intell. Fuzzy Syst.*, vol. 25, no. 2, pp. 505–515, 2013.
[39] M. Ester, H. Kriegel, J. Sander, and X. Xu, "A density-based algorithm for discovering clusters in large spatial databases with noise," in *Proc. 2nd Int. Conf. Knowl. Discov. Data Mining*, 1996, pp. 226–231.
[40] W. Pedrycz, "Shadowed sets: Representing and processing fuzzy sets," *IEEE Trans. Syst., Man Cybern.*, vol. 28, no. 1, pp. 103–109, Feb. 1998.
[41] X. F. Deng and Y. Y. Yao, "Decision-theoretic three-way approximations of fuzzy sets," *Inf. Sci.*, vol. 279, pp. 702–715, 2014.
[42] X. F. Deng and Y. Y. Yao, "Mean-value-based decision-theoretic shadowed sets," in *Proc. Joint IFSA world Congr. NAFIPS Annu. Meeting*, 2013, pp. 1382–1387.
[43] D. R. Wu and J. M. Mendel, "A comparative study of ranking methods, similarity measures and uncertainty measures for interval type-2 fuzzy sets," *Inf. Sci.*, vol. 179, no. 8, pp. 1169–1192, 2009.
[44] J. Xu, G. Y. Wang, and W. H. Deng, "Denpehc: Density peak based efficient hierarchical clustering," *Inf. Sci.*, vol. 373, pp. 200–218, 2016.
[45] C. Merz, "UCI repository of machine learning databases," 1996. [Online]. Available: https://archive.ics.uci.edu
[46] D. Lapp, "Heart disease dataset," 2019. [Online]. Available: https://www.kaggle.com/datasets/johnsmith88/heart-disease-dataset/data
[47] J. Derrac, S. Garcia, L. Sanchez, and F. Herrera, "Keel data-mining software tool: Data set repository, integration of algorithms and experimental analysis framework," *J. Mult. Valued Logic Soft Comput.*, vol. 17, pp. 255–287, 2015.
[48] Q. Xie et al., "GBG++: A fast and stable granular ball generation method for classification," *IEEE Trans. Emerg. Topics Comput. Intell.*, vol. 8, no. 2, pp. 2022–2036, Apr. 2024, doi: 10.1109/TETCI.2024.335909.